

## 2. Multifractal Analysis

The single-day profile  $U_\nu$  is defined by the cumulation of single-window (local) mean interevent times  $\overline{\Delta t}_i^\nu$ :  $U_\nu(i) = \sum_{i'=1}^i \overline{\Delta t}_{i'}^\nu$ , which defines a directed (climbing) random walk (index  $i$  is defined in the paragraph below).

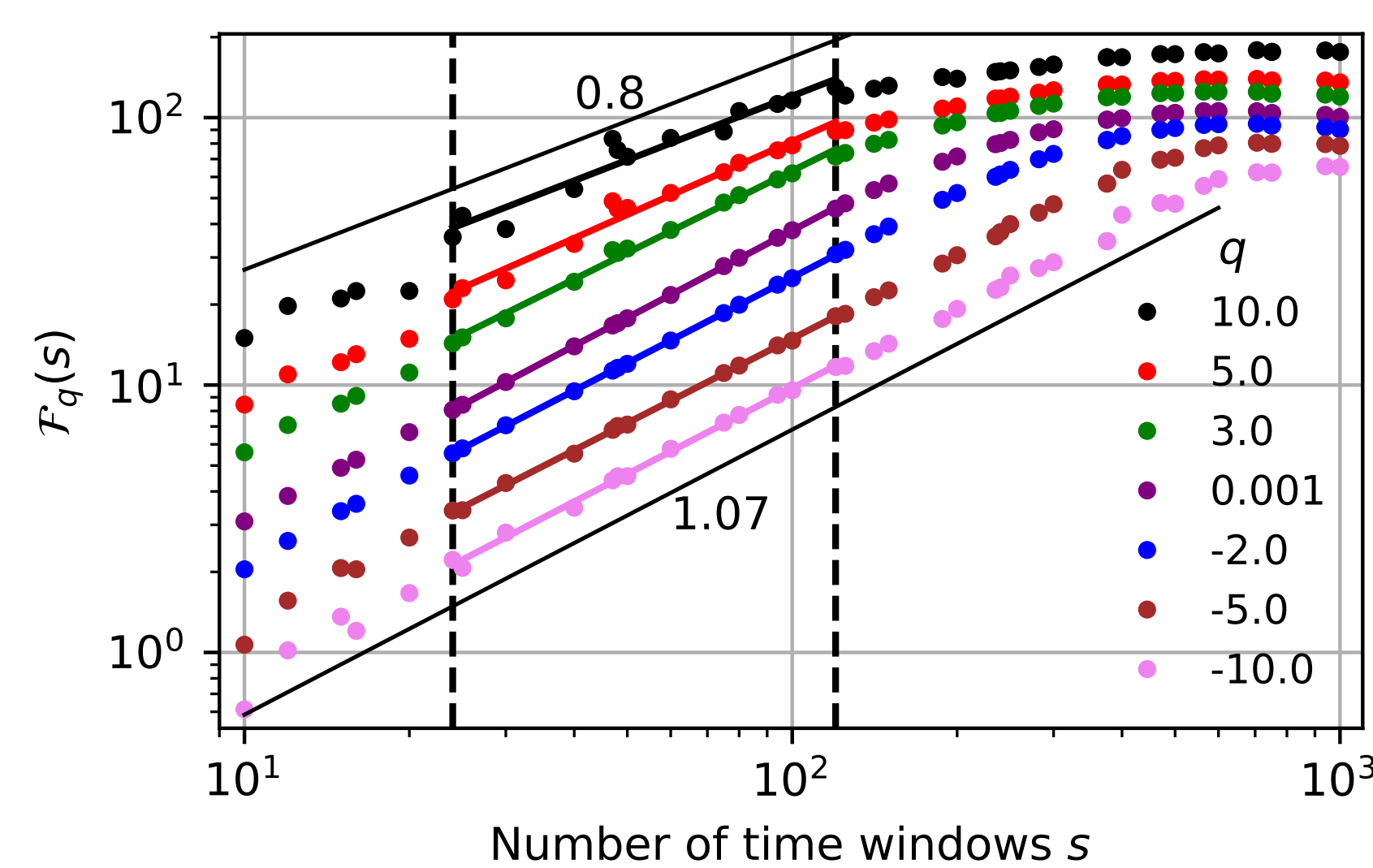
The intraday autocorrelation of the absolute detrended profile is defined for a single day  $\nu$  and a given time scale  $s$ ,

$$F^2(j; \nu, s) = \frac{1}{s-j} \sum_{i=1}^{s-j} |U(i+j) - y_\nu(i+j)| \cdot |U(i) - y_\nu(i)|, \quad \nu = 1, \dots, N_d,$$

where  $j = 0, \dots, s-1$ , defines time-step distance or number of time windows of length  $\Delta$  between both absolute deviations (detrended fluctuations)  $|U_\nu - y_\nu|$  present at day  $\nu$  at time steps  $i$  and  $i+j$  ( $1 \leq i \leq s$  numbers the current time window),  $s$  is the total number of time windows within a single replica  $\nu$ ,  $1 \leq \nu \leq N_d$ , and  $N_d$  is the number of trading days. Apparently, for  $j=0$  the detrended autocorrelation function becomes a detrended fluctuation function. Therefore, we can introduce the notation  $F^2(\nu, s) = F^2(0; \nu, s)$ .

Generalized Hurst exponent  $h(q)$  can be estimated using the  $q$ -dispersive function  $\mathcal{F}_q(s)$

$$\mathcal{F}_q(s) = \left( N_d^{-1} \sum_{\nu=1}^{N_d} [F^2(\nu; s)]^{q/2} \right)^{1/q}, \quad \ln \mathcal{F}_q(s) \approx h(q) \ln(s) + B(q).$$



On the left, there are plots of  $\mathcal{F}_q(s)$  vs  $s$  in the log-log scale for empirical data for different values of  $-10 \leq q \leq 10$ . Vertical dashed lines define the region of scaling, where  $h(q)$  can be estimated.

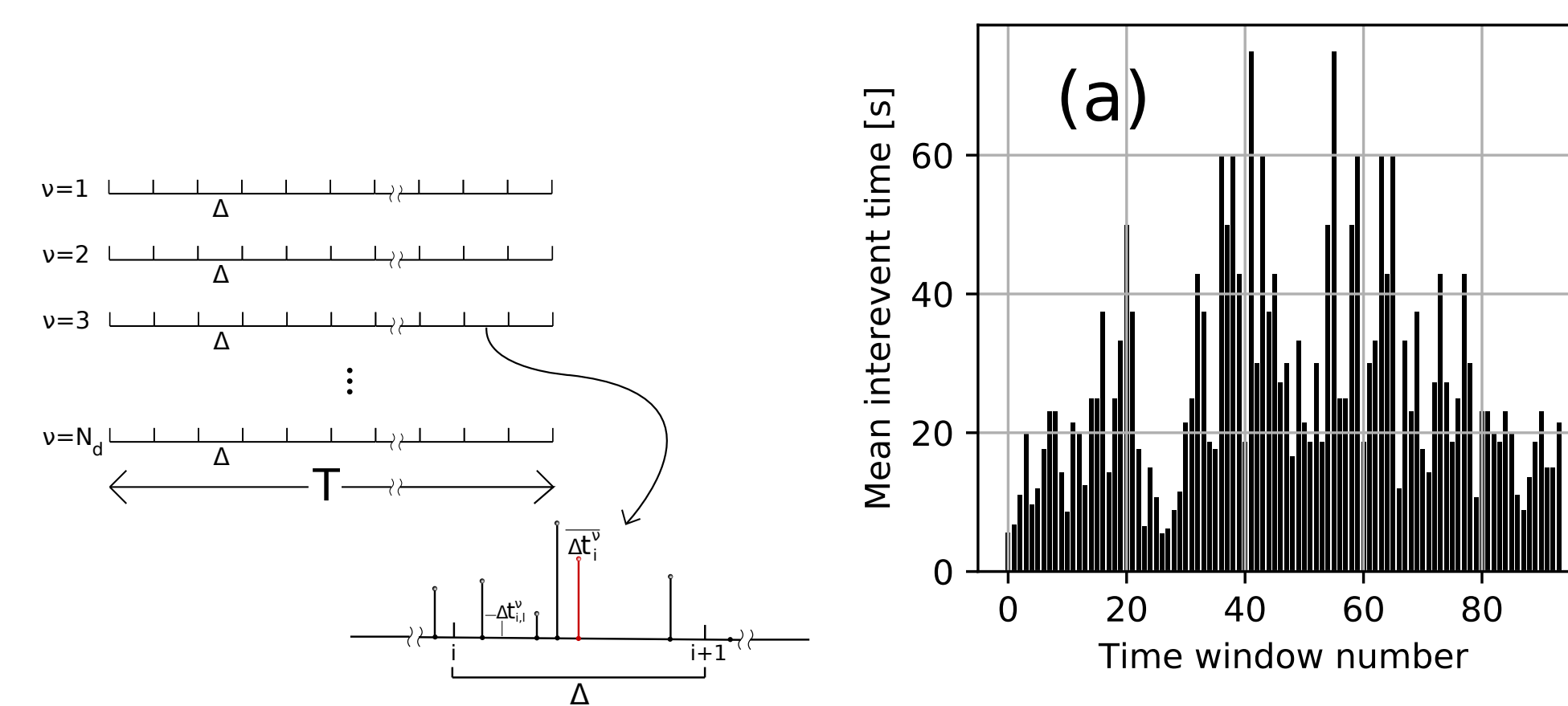
Finally, we can calculate Rényi scaling exponent  $\tau(q)$  and the spectrum of singularities using the Legendre-Fenchel transformation:

$$\tau(q) = qh(q) - h(q=1), \quad \alpha(q) = \frac{d\tau(q)}{dq}, \quad f(\alpha(q)) = q\alpha(q) - \tau(q),$$

where  $\alpha$  is a local dimension (singularity or Hölder exponent), while  $f(\alpha)$  is its distribution. For the monofractal structure the scaling exponent  $\tau(q)$  is a linear function of  $q$ , while for multifractal it is the non-linear one.

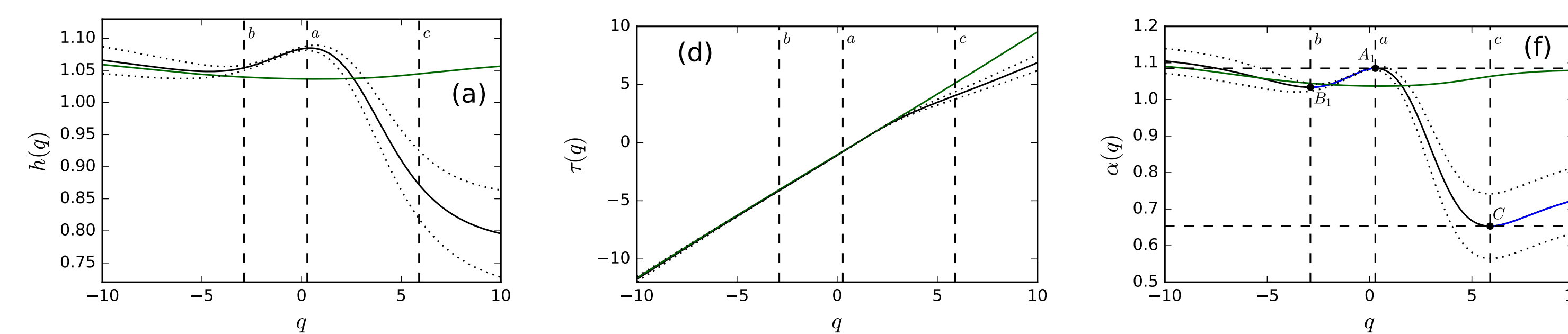
We can also calculate specific heat  $c(q) = -q^2 \frac{d\alpha(q)}{dq}$ , used to investigate thermal stability.

## 1. Intraday Activity

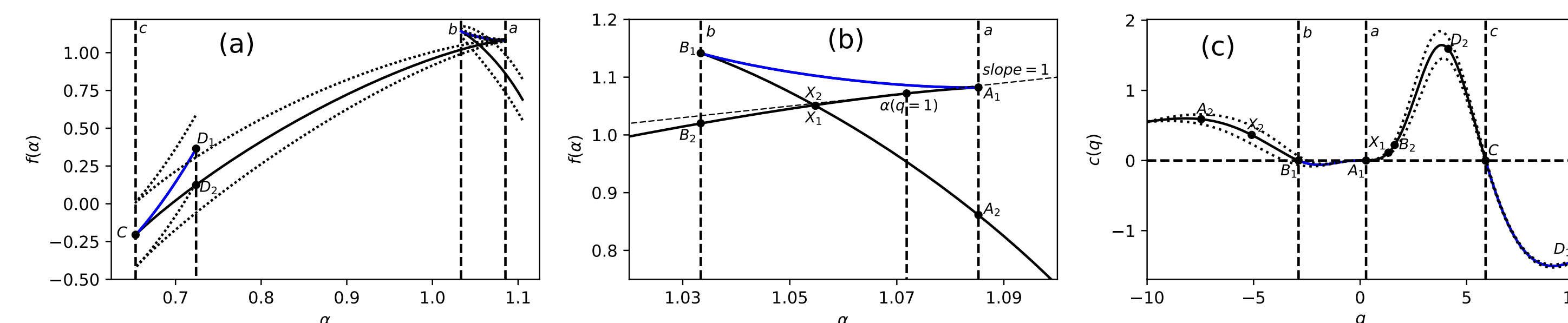


Activity of market participants varies during trading hours. Mean time between transactions is the lowest at the beginning and ending of the trading, and is the highest in the middle. This lunch effect is a signature of the non-stationarity of the price process. We split trading day into windows of length  $\Delta$  and calculate mean intertrade time in every window. The scheme of the procedure is shown in the left figure. We use financial tick-by-tick data for KGHM - one of the most liquid stock from Warsaw Stock Exchange. The right graph presents result for the exemplary day using 5-minute time windows. Non-stationarity can be clearly seen. Typically, local clusters of spikes around their local maximums are well visible. We observe the highest maxima in the vicinity of the lunch time. Such a long-term structure constitutes a source of generalized "volatility clustering" of detrended interevent times' series fluctuations and hence their multifractality.

## 3. Multifractal Spectra

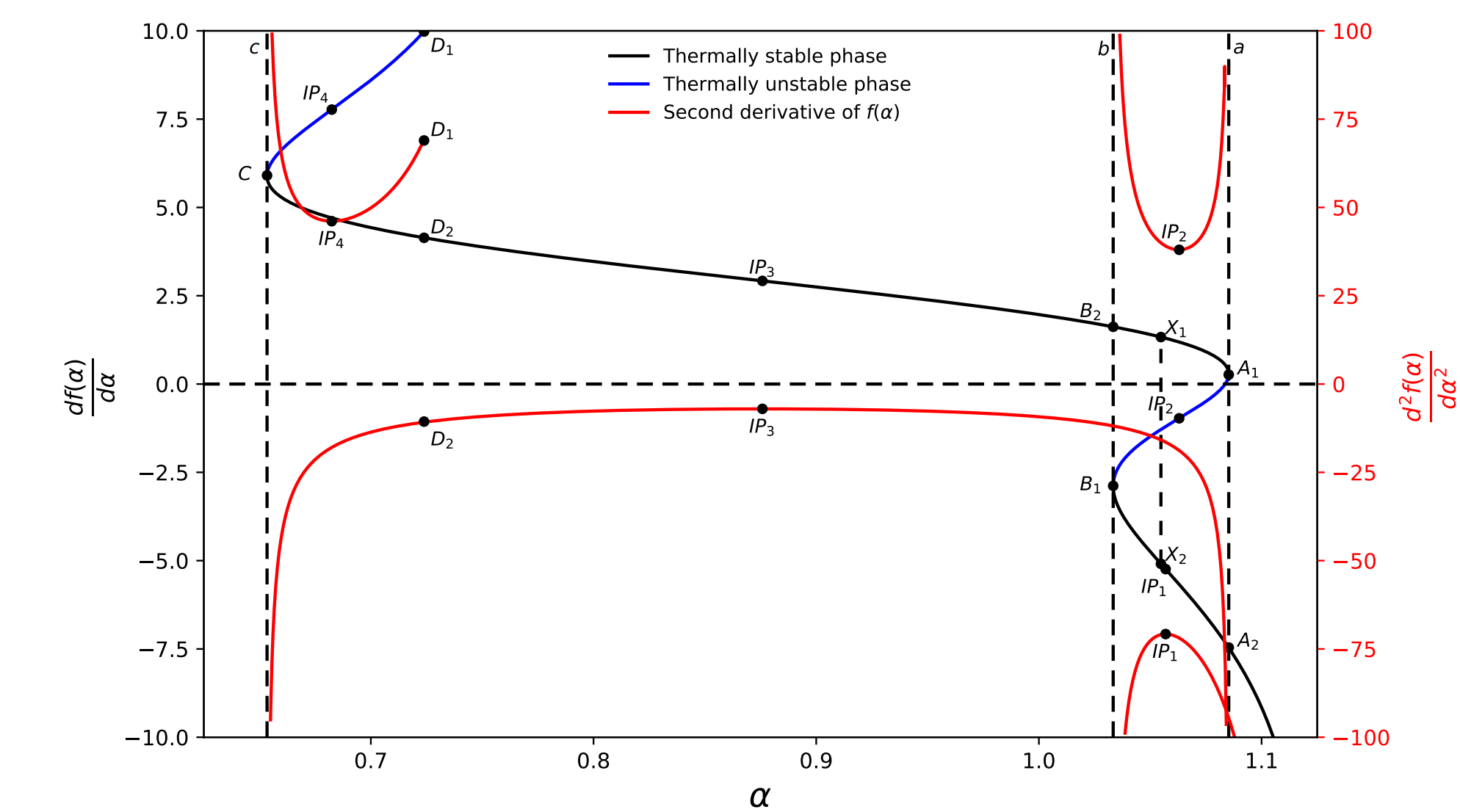


The  $q$ -dependence of main characteristics of multifractality. The nonlinear dependence of these characteristics on  $q$  is well seen. Plots present dependence on  $q$  of the generalized Hurst exponent  $h(q)$ , Rényi scaling exponent  $\tau(q)$  and the coarse Hölder exponent  $\alpha(q)$ , respectively. Additional dark green solid curves presented on all plots were obtained from the time series generated by the Poisson process. Apparently, their variations are negligible which means that the influence of a finite size effect on a time series with a size equal to the empirical one is negligible.



Plots (a) and (b) are different views of spectrum of dimensions  $f(\alpha)$  vs  $\alpha$ , and (c) is specific heat  $c(q)$  vs  $q$ . Vertical lines marked by  $a$  and  $c$  define the range of  $q$  where peak  $c(q) \geq 0$  that is, the range of thermal stability of the part of the system defined by the main (longest, increasing) branch of spectrum of dimensions. Apparently, also the side branch containing points  $B_1$  and  $A_2$  is thermally stable. Notably, at turning points  $A_1, B_1, C$  the second order phase transitions occur. The vertical dashed line displayed on plot (b) in point  $\alpha(q=1)$ , determines the position of the tangent dashed straight line with a slope of 1.0 for the main branch. This is a verification of the contact character of the L-F transform, which obeys:  $f(\alpha(q=1)) = \alpha(q=1)$  and  $\frac{df(\alpha)}{d\alpha} |_{q=1} = 1.0$ .

## 4. Phase Transitions



The illustration of the Ehrenfest like classification of phase transitions. The first (black and blue solid curve) and second (four separated red solid curves) derivatives of  $f$  over  $\alpha$  showing three two-branched second order singularities of  $f$  vs  $\alpha$ . Three dashed vertical straight lines (vertical asymptotics)  $c, b$ , and  $a$  are located, indeed, at  $\alpha$  coordinates of singularities. The main branch of derivative  $df/d\alpha$  is represented by the black and blue curve ( $C, D_2, B_2, X_1, A_1$ ) containing also the inflection point  $IP_3$ . The corresponding red curve of the second derivative  $d^2f/d\alpha^2$  contains the replica of the inflection point  $IP_3$  which diverges at asymptotics  $c$  and  $a$ . This curve is singular at turning points: the left one at  $\alpha$  coordinate of point  $C$  and the right one at  $\alpha$  coordinate of point  $A_1$ . The other three singular curves (also in red) are associated with three side branches of the first derivative  $df/d\alpha$ .

## 5. References

- [1] J. W. Kantelhardt, S. A. Zschiegner, E. Kościelny-Bunde, A. Bunde, S. Havlin, and H. E. Stanley, Physica A 316, 87 (2002).
- [2] P. Oświęcimka, J. Kwapien, S. Drożdż, Phys. Rev. E, 74 (2006), p. 016103
- [3] J. Perelló, J. Masoliver, A. Kasprzak, R. Kutner, Phys. Rev. E, 78 (2008), p. 036108
- [4] J. Klamut, T. Gubiec, R. Kutner, Z. R. Struzik, **Multi-branch multifractality and the phase transitions in time series of mean interevent times**, Phys. Rev. E 101 (2020), 063303